

Relevance of Protein Content within the Renal Scaffold for Kidney Bioengineering and Regeneration

Fatima Guerrero¹, Andres Carmona¹, Rosa Ortega^{1,2}, Sagrario Cañadillas^{1,3}, Rodolfo Crespo^{4,5}, Concha Herrera^{1,3,5,6}, Pedro Aljama^{1,4,5,7}

¹Maimonides Institute of Biomedical Research of Cordoba, Cordoba, Spain; ²Anatomical Pathology Service, Reina Sofia University Hospital, Cordoba, Spain; ³Cellular Therapy Unit, Reina Sofia University Hospital, Cordoba, Spain; ⁴Department of Nephrology, Nephrology Service, Reina Sofia University Hospital, Cordoba, Spain; ⁵University of Cordoba, Cordoba, Spain; ⁶Hematology Department, Reina Sofia University Hospital, Cordoba, Spain; ⁷RETICs Red Renal, Instituto de Salud Carlos III, Madrid, Spain

Correspondence to: Fatima Guerrero, fatima.guerrero@imibic.org

Keywords: Bioengineering, Kidney, Decellularization, Scaffold, Proteomic

Received: September 29, 2017

Accepted: November 26, 2017

Published: November 29, 2017

Copyright © 2017 by authors and Scientific Research Publishing Inc.

This work is licensed under the Creative Commons Attribution International License (CC BY 4.0).

<http://creativecommons.org/licenses/by/4.0/>



Open Access

ABSTRACT

Chronic kidney disease is currently a major public health problem around the world. Although hemodialysis increases survival of patients with end-stage renal disease, kidney transplantation remains the only potentially curative treatment. However, transplantation as a therapeutic option is limited by availability of suitable donor organs. This situation highlights the urgent need to find new and potentially inexhaustible sources of transplantable organs. Perfusion decellularization of whole organs is a novel approach to organ engineering and regeneration. In the present research, we used a continuous perfusion decellularization protocol to eliminate cellular component of kidney and evaluated residual scaffold components after decellularization process by proteomics analysis. Our proteomic data show that this protocol results in incomplete removal of cellular proteins. However, unlike other authors, we assume that proteins retained within decellularized kidney scaffold could be the basis for specific homing and cellular differentiation in the recellularization process.

1. INTRODUCTION

Chronic kidney disease (CKD) is currently a major public health worldwide problem [1, 2]. CKD affects a significant percentage of the population; mainly due to that their leading causes are highly prevalent disorders such as aging, hypertension, diabetes and vascular disease [3]. Although hemodialysis increases survival of patients with end-stage renal disease (ESRD), the kidney transplantation remains the only po-

tentially curative treatment [4]. Because of this, the demand for suitable organs for transplantation has reached a level that far exceeds supply. This disparity has greatly to a wide waiting list. These data highlight the urgency to find new and potentially inexhaustible sources of transplantable organs.

Tissue engineering and regenerative medicine arise as a promising solution for the treatment of kidney disease through the development of renal structures with normal function by bioengineering. Recent advances in this area, involving decellularization of native organs and further recellularization of the resulting extracellular matrix (ECM), have provided a hopeful approach for the production of transplantable organs [5-10].

Kidney decellularization has been successfully achieved using a variety of approaches and protocols. Currently, the most efficient technique that allows decellularization of complete organs is the chemical perfusion. Sodium dodecyl sulfate (SDS) and non-ionic detergent Triton X-100, are the most frequently used agents for tissue decellularization [5, 11-14]. These agents allow complete removal of cellular material, preserving the three-dimensional ECM and vascular network within the organ.

Criteria to evaluate the effectiveness of the decellularization process are mainly based on structural and content details of the ECM scaffold by both histological and biochemical analysis. However, recent observations underwrite that decellularized scaffolds still contain many cellular protein and proteomic analysis would provide crucial characterization of the decellularization process to create scaffolds bio-compatible, nontoxic and suitable for its subsequent recellularization [15].

In this research, our aims were 1) to develop decellularization protocol by detergent perfusion that effectively removes all cellular components of the kidney and 2) to assess the changes in the proteome after decellularization process.

2. METHODS

2.1. Harvesting of Rat Kidneys

All experimental protocols were reviewed and approved by the Ethics Committee for Animal Research of the University of Cordoba, and all rats received humane care in compliance with the guiding principles in the Guide for the Care and Use of Laboratory Animals.

The animals were sacrificed by exsanguination under general anaesthesia (i.p. sodium thiopental). After a median laparotomy and systemic heparinization through the infrahepatic inferior vena cava for anticoagulation, renal artery, renal vein and ureter were completely isolated. Subsequently, the whole kidney was harvested and transferred to a cell culture dish. The whole kidney was maintained hydrated with cooled PBS while the main vasculature of the organ was cannulated.

2.2. Whole-Organ Perfusion Decellularization

We performed a decellularization protocol following the method used by Guyette J *et al.* [11], with minor modifications. Briefly, renal artery was cannulated with a 24-G cannula and fixed with 3/0 silk suture. The kidney was manually perfused with 10 ml of diluted heparin (Sanofi, Gentilly, France) solution to remove residual blood. Then, the cannulated kidney was mounted into the decellularization chamber and was connected to the peristaltic pump (Fresenius-Kabi, Bad Homburg, Germany). The perfusion rate for each step was set at 0.4 mL/min. The decellularization process was initiated by perfusion with PBS for 30 minutes, followed by 0.66% SDS (Thermo Fisher Scientific, Waltham, MA, USA) in deionized water for 18 hours until organ translucency was confirmed. Finally, the kidney was perfused with 1% Triton X-100 (Acros Organics, Fisher Scientific) in deionized water for 30 minutes. Following decellularization, we washed the kidney scaffolds with PBS containing 10,000 U/mL penicillin G, 10 mg/mL streptomycin, and 25 µg/mL amphotericin-B (Sigma-Aldrich, St. Louis, MO, USA) at 0.4 mL/min constant arterial perfusion for 96 hours. Wash solution was changed every 12 hours.

All used solutions were buffered at pH 7.4 and prepared under sterile conditions. The buffered solutions were kept to 4°C until used.

2.3. Visualization of the Vascular System

To visualize the three-dimensional microvasculature in the scaffolds after decellularization, a blue colored solution was injected through cannulated renal artery of the decellularized kidney. To perform the solution was used Commassie Brilliant Blue R (Sigma-Aldrich).

2.4. Quantification of Residual Detergent

Removal of SDS detergent of the kidney perfusate solution was quantified using the Stains All Dye reagent (Sigma-Aldrich) by absorbance readings at 438 nm as previously described by Rusconi F *et al.* [16].

2.5. Basic Histology Assessment of the Kidney Scaffolds

To assess cell and nuclear clearance as well as preservation of extracellular matrix, hematoxylin and eosin (H&E) and silver methamine staining were performed in decellularized and native kidneys. Briefly, decellularized and native kidneys transverse sections were fixed in 4% formalin, dehydrated through a graded series of ethanol, and embedded in paraffin. Three-micrometer paraffin sections were stained with H&E and methenamine silver and examined by normal light microscopy.

2.6. Protein Extraction and Digestion

Protein lysates from native and decellularized kidney were prepared by homogenizing tissue in lysis buffer (7 M urea, 4% CHAPS (w/v), 0.5 M DTT) containing protease inhibitor cocktail (Sigma-Aldrich) using a rotating blade homogenizer. Samples were cleaned by protein precipitation with TCA/acetone and solubilised in 50 μ L of 0.2% RapiGest SF (Waters, Milford, MA, USA) in 50 mM ammonium bicarbonate. The total protein content was measured using the Qubit Protein Assay Kit (Thermo Fisher Scientific); 50 μ g of protein was subjected to trypsin digestion following a protocol adapted from Vowinckel *et al.* [17]. Briefly, protein samples were incubated with 5 mM DTT at 60°C for 30 min and then with 10 mM iodoacetamide at room temperature and in darkness for 30 min. Sequencing Grade Modified Trypsin (Promega, Madison, WI, USA) was added at a 1:40 trypsin:protein ratio and incubated at 37°C for 2 hours; the same amount of trypsin was again added and incubated at 37°C for another 15 hours. RapiGest was then precipitated by centrifugation after incubating with 0.5% TFA at 37°C for 1 hour.

2.7. Mass Spectrometry Analysis

The peptide solutions were analysed by a shotgun data-dependent acquisition (DDA) approach using nano-LC-MS/MS. One μ g of each pooled sample (2 μ L) was separated into a nano-LC system Eksport nLC415 (Eksigent, Dublin, CA, USA) using an Acclaim PepMap C18 column (75 μ m \times 25 cm, 3 μ m, 100 Å) (Thermo Fisher Scientific) at a flow rate of 300 nl/min. Water and ACN, both containing 0.1% formic acid, were used as solvents A and B, respectively. The gradient run consisted of 5% to 30% B for 120 min.

Eluting peptides were directly injected into a hybrid quadrupole-TOF mass spectrometer Triple TOF 5600+ (Sciex, Redwood City, CA, USA) operated with a data-dependent acquisition system in positive ion mode. A NanoSpray III ESI source (Sciex) was used for the interface between nLC and MS, with an application of 2600 V voltage. The acquisition mode consisted of a 250 ms survey MS scan from 350 to 1250 m/z followed by an MS/MS scan from 230 to 1700 m/z (60 ms acquisition time, rolling collision energy) of the top 65 precursor ions from the survey scan, for a total cycle time of 4.2 s. The fragmented precursors were then added to a dynamic exclusion list for 15 s; any singly charged ions were excluded from the MS/MS analysis.

The peptide and protein identifications were performed using Protein Pilot software (version 5.0.1, Sciex) with a Rattus Swiss-Prot concatenated target-reverse decoy database (downloaded in May 2015), containing 7927 target protein sequences, specifying iodoacetamide as Cys alkylation. The false discovery

rate (FDR) was set to 0.01 for both peptides and proteins.

2.8. GO Analysis and Bioinformatic Tools

The proteins identified in native and kidney scaffold were described using Uniprot knowledgebase (<http://www.uniprot.org/>). The list of gene names from each dataset was used to generate a Venn diagram (<http://bioinformatics.psb.ugent.be/webtools/Venn/>). Network analysis protein-protein interactions of the identified proteins were performed using STRING (<https://string-db.org/>). The confidence score for selection was 0.7. Gene ontology (GO) terms enrichment was calculated using Gene Ontology enRIchment anaLysis and visuaLizAtion (GORilla) tool (<http://cbl-gorilla.cs.technion.ac.il/>). Significance for each GO term was assessed with p-values that were corrected using FDR q-value according to the Benjamini and Hochberg (1995) method.

3. RESULTS

3.1. Kidney Decellularization

In our laboratory, the continuous perfusion decellularization protocol was based on the combination of two detergents (SDS and Triton X-100). Detergent perfusion and washing of rat kidney was maintained with low and constant physiological perfusion pressures to allow gradual adaptation to changes in vascular resistance. As shown in the **Figure 1(A)** & **Figure 1(B)**, after decellularization of rat kidney, the scaffold

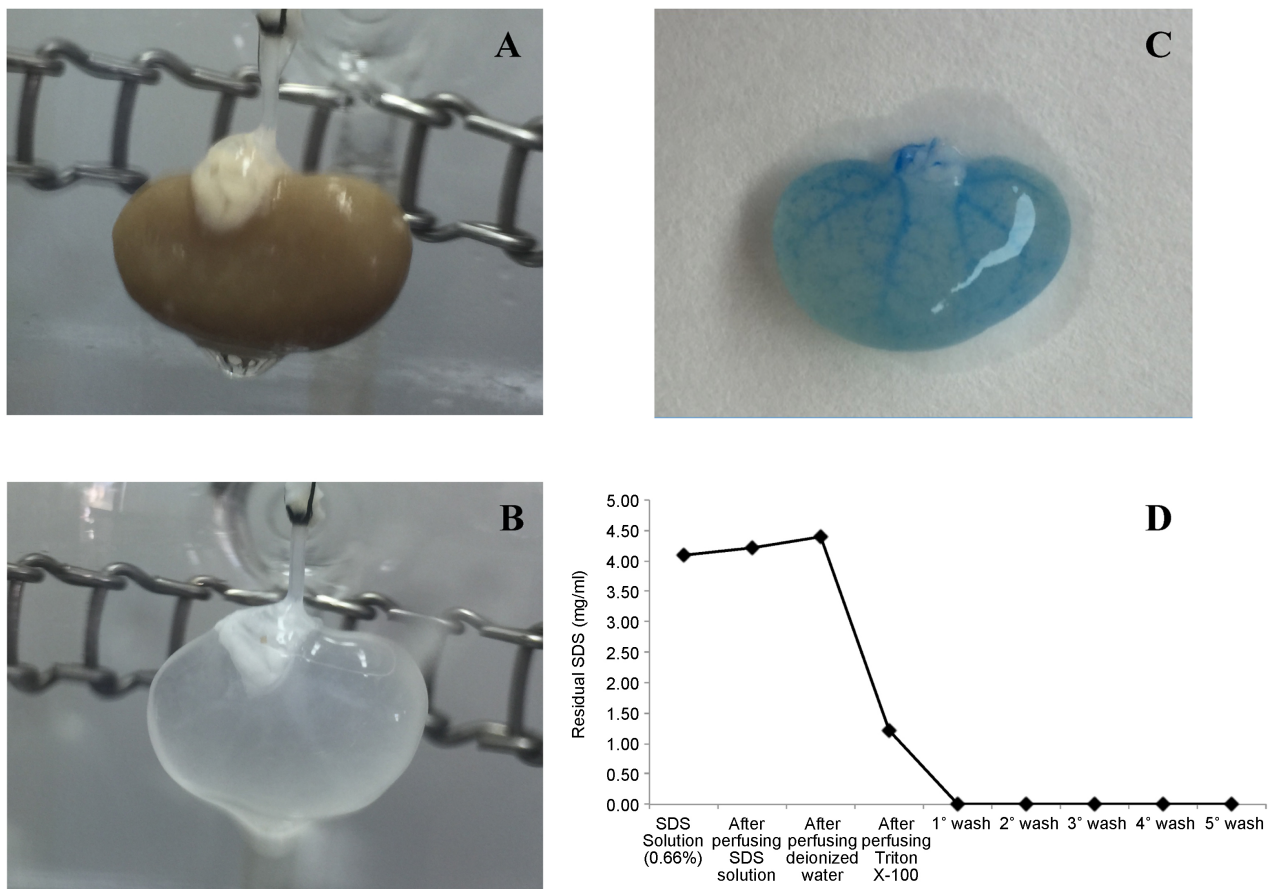


Figure 1. Representative pictures of kidney (A) before and (B) after decellularization process. Mean length of native and scaffold kidney was 1.8 cm. (C) Visualization of the vascular network. (D) SDS quantification in kidney perfusate solutions.

retained overall shape and the macroscopic structure, and became white and translucent due to the removal of the cellular contents. Furthermore, the three dimensional structure of the vasculature was preserved and intact (**Figure 1(C)**).

According to previous studies, SDS perfusion shows severe cellular toxicity in subsequent recellularization processes [11, 18]. Analysis of several samples of the perfusate solution during decellularization process confirmed removal of SDS detergent. After perfusing Triton-X100, we observed a marked decrease in the levels of SDS becoming undetectable in the washing process, suggesting complete removal of residual SDS (**Figure 1(D)**).

3.2. Histological Characterization of the Rat Renal ECM Scaffold

The microscopic examination revealed the renal scaffold microarchitecture preserved and the integrity of the glomerular, tubular and vascular structures. Histologic evaluation with H&E staining showed pink eosinophilic structures typical of collagen fibrils, whereas no basophilic staining typical of cellular nuclear material was observed (**Figure 2(E)**), as compared to normal rat kidney staining (**Figure 2(B)**).

Moreover, methenamine silver staining was performed to assess preservation of basement membranes. **Figure 2(F)** showed the characteristic pattern (in black) of the glomerular and tubular basement membranes intact after the decellularization process and confirming successfully eliminate the cellular component compared to normal rat kidney staining (**Figure 2(C)**).

3.3. Proteomic Analysis of the Kidney Scaffold

The proteins identified in native and kidney scaffold were described using Uniprot knowledgebase (Data Supplementary). As expected, fewer distinct proteins were detected after decellularization process,

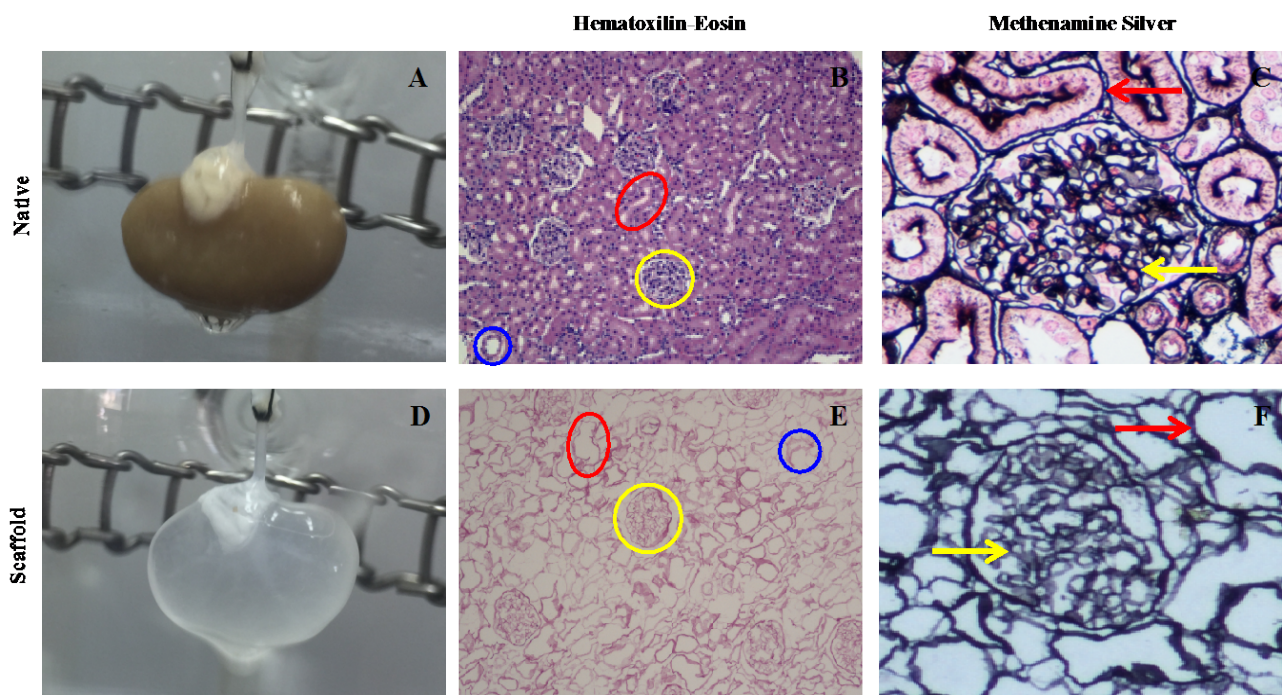
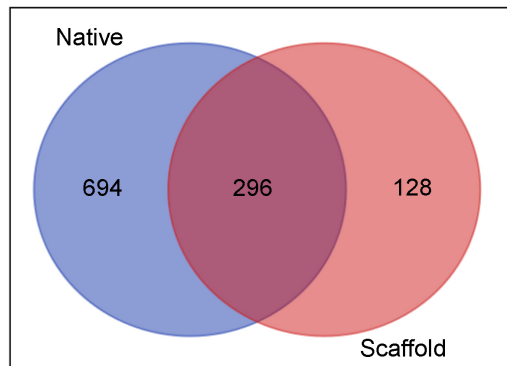
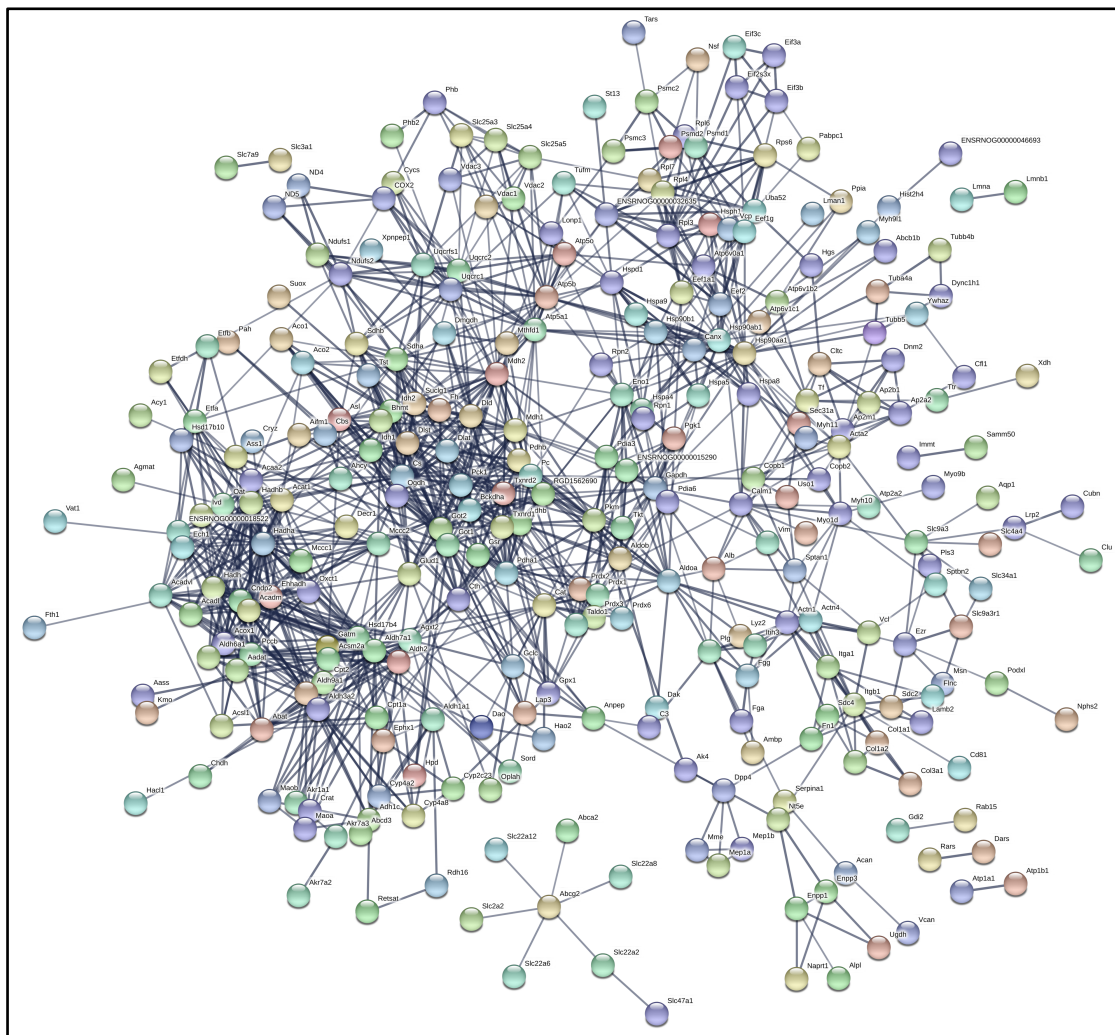


Figure 2. Histological analysis of renal scaffold. ((B), (E)) H&E staining of native (B) versus decellularized kidney (E). Circles show glomerular (yellow), tubular (red) and vascular (blue) structures. ((C), (F)) Methenamine silver staining of native (C) versus decellularized kidney (F). Arrows show glomerular (yellow) and tubular (red) basement membranes.

dropping from 990 to 424 proteins identifications in the native and decellularized kidney respectively. As shown in the Venn Diagram (**Figure 3(A)**), of the total 424 proteins identified after decellularization



(A)



(B)

Figure 3. (A) Venn diagram with the number of protein identifications for native and decellularized kidney; (b) protein interaction map of proteins identified in the renal scaffold.

process, 296 proteins were conserved to both native and kidney scaffold and 128 were exclusively represented in renal scaffold (Data Supplementary). Figure 3(B) shows the interaction network of the proteins with high confidence. The interactions among themselves indicates that the proteins are biologically connected.

GORilla tool using a single ranked list of genes was performed to analyze the cellular component ontology in the decellularized rat kidney. The system recognized 421 genes out of 424 gene terms entered, only 419 of these genes were associated with a GO term. The results revealed 20 GO terms enriched for cellular component (Figure 4, Table 1). Some highly enriched cellular component terms were associated to protein complex and ECM. Associated genes for extracellular matrix term (GO:0031012) are shown in the Table 2. Each gene name is specified by gene symbol followed by a short description of the gene.

Table 1. GO classification of enriched cellular component.

GO term	Ontology	Description	p-Value	FDR q-value	Enrichment
GO:0043209	Cellular Component	myelin sheath	2.24E-5	1.46E-2	1.96
GO:0043234	Cellular Component	protein complex	4.75E-5	1.55E-2	2.43
GO:0031012	Cellular Component	extracellular matrix	6.79E-5	1.47E-2	1.91
GO:0030863	Cellular Component	cortical cytoskeleton	1.07E-4	1.74E-2	35.91
GO:0030139	Cellular Component	endocytic vesicle	1.3E-4	1.69E-2	34.92
GO:0098862	Cellular Component	cluster of actin-based cell projections	1.96E-4	2.13E-2	16.76
GO:0005903	Cellular Component	brush border	1.96E-4	1.82E-2	16.76
GO:0043231	Cellular Component	intracellular membrane-bounded organelle	2.68E-4	2.18E-2	1.24
GO:0005759	Cellular Component	mitochondrial matrix	2.82E-4	2.04E-2	1.37
GO:0005768	Cellular Component	endosome	3.59E-4	2.33E-2	10.07
GO:0044448	Cellular Component	cell cortex part	3.78E-4	2.23E-2	27.93
GO:0043233	Cellular Component	organelle lumen	4.41E-4	2.39E-2	1.90
GO:0031974	Cellular Component	membrane-enclosed lumen	4.41E-4	2.21E-2	1.90
GO:0005911	Cellular Component	cell-cell junction	5.21E-4	2.42E-2	13.97
GO:0005774	Cellular Component	vacuolar membrane	5.68E-4	2.47E-2	5.72
GO:0012506	Cellular Component	vesicle membrane	6.23E-4	2.54E-2	12.89
GO:0005739	Cellular Component	mitochondrion	7.2E-4	2.76E-2	1.31
GO:0098852	Cellular Component	lytic vacuole membrane	8.46E-4	3.06E-2	8.80
GO:0005765	Cellular Component	lysosomal membrane	8.46E-4	2.9E-2	8.80
GO:1990204	Cellular Component	oxidoreductase complex	9.09E-4	2.96E-2	2.54

Table 2. Associated genes for extracellular matrix term (GO:0031012).

Germ	Description
Vim	vimentin
Agrn	agrin
Lmna	lamin a/c
Rpn1	ribophorin i
Canx	calnexin
Dync1h1	dynein cytoplasmic 1 heavy chain 1
Alpl	alkaline phosphatase, liver/bone/kidney
Eef2	eukaryotic translation elongation factor 2
Hspa8	heat shock 70 kda protein 8
Myh9	myosin, heavy chain 9, non-muscle
Hspa9	heat shock protein 9
Hsp90b1	heat shock protein 90, beta, member 1
Prdx1	peroxiredoxin 1
Hspa5	heat shock protein 5
Tubb5	tubulin, beta 5 class i
Hadha	hydroxyacyl-coa dehydrogenase/3-ketoacyl-coa thiolase/enoyl-coa hydratase (trifunctional protein), alpha subunit
Col1a2	collagen, type i, alpha 2
Nid2	nidogen 2 (osteonidogen)
Nid1	nidogen 1
Col1a1	collagen, type i, alpha 1
Cltc	clathrin, heavy chain (hc)
Clu	clusterin
Atp5a1	atp synthase, h+ transporting, mitochondrial f1 complex, alpha subunit 1, cardiac muscle
Hspd1	heat shock protein 1 (chaperonin)
Slc25a5	solute carrier family 25 (mitochondrial carrier; adenine nucleotide translocator), member 5
Atp5b	atp synthase, h+ transporting, mitochondrial f1 complex, beta polypeptide
Lamb2	laminin, beta 2
Fn1	fibronectin 1
Vcan	versican

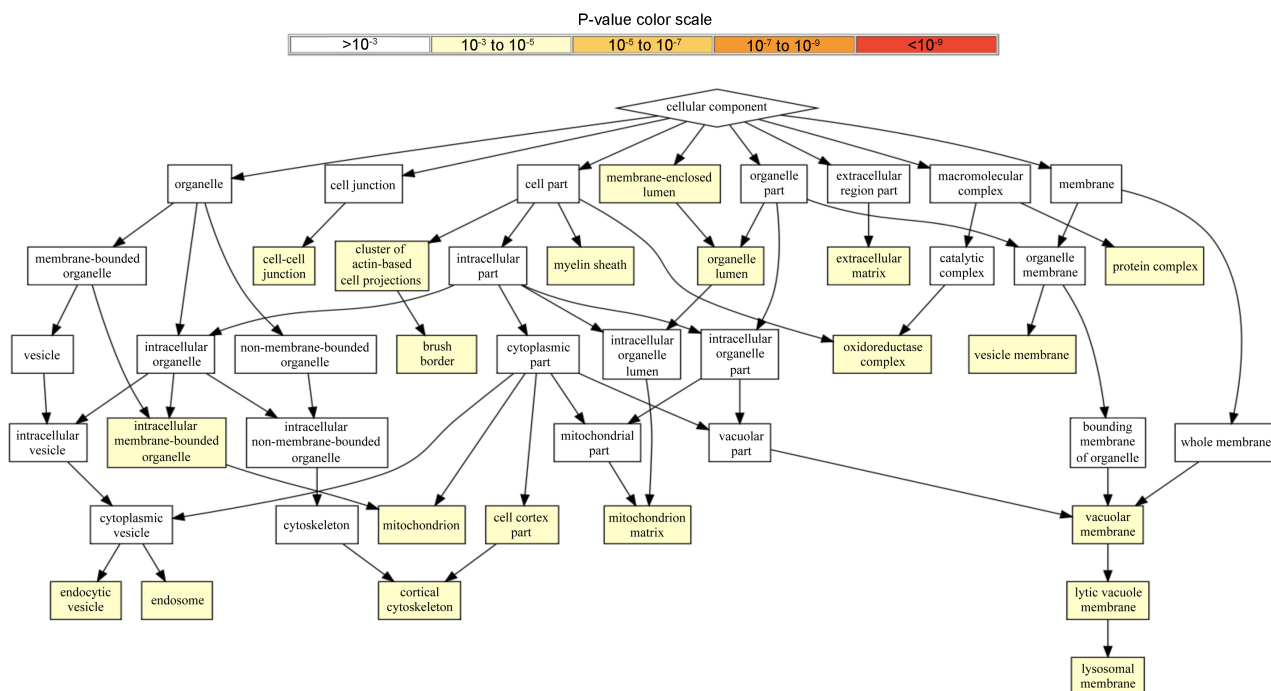


Figure 4. GO classification of enriched cellular component in renal scaffold.

Proteins were subsequently categorized into their functional and biological processes. GOrilla tool using two unranked lists of genes (scaffold as target list and native as background list) was performed. The system recognized 1404 genes out of 1414 gene terms entered, only 1092 of these genes were associated with a GO term. The results revealed 2 GO terms enriched for molecular function (Figure 5, Table 3) and 3 GO terms enriched for biological process (Figure 6, Table 4).

The biological process terms identified were related to metabolic process including organic acid metabolic process (GO:0006082), oxoacid metabolic process (GO:0043436) and carboxylic acid metabolic process (GO:0019752). Several enrichment molecular function terms were related to cofactor binding (GO:0048037) and secondary active transmembrane transporter activity (GO:0015291).

4. DISCUSSION

Renal transplantation is currently the most effective treatment for ESRD that represents one of the primary mortality reason globally. Because of this, the demand for transplantable organs continues to grow and the number of available organs seems to have plateaued in recent years. Consequently, there is a urgent need to identify new, potentially inexhaustible sources of clinically applicable and transplantable kidneys.

Perfusion decellularization of whole organs is a novel approach to organ engineering and regeneration. The use of a decellularized kidney scaffold is based on the mechanical and biological property of the ECM, which can maintain natural cellular architecture and some residual molecules that may advantage recellularization, differentiation and proliferation of the host cells. Kidney decellularization has been successfully achieved using a variety of approaches and protocols. Recently, Destefani *et al.* showed a comprehensive investigation about different protocols for rat kidney decellularization [19]. Although, to date no specific protocol has demonstrated to be superior to the others.

In this study, the continuous perfusion decellularization protocol was based on the combination of two detergents (SDS and Triton X-100). We perfused kidneys using a peristaltic pump to ensure monitoring of perfusion pressure. Perfusion pressure was maintained in physiological range (up to 120

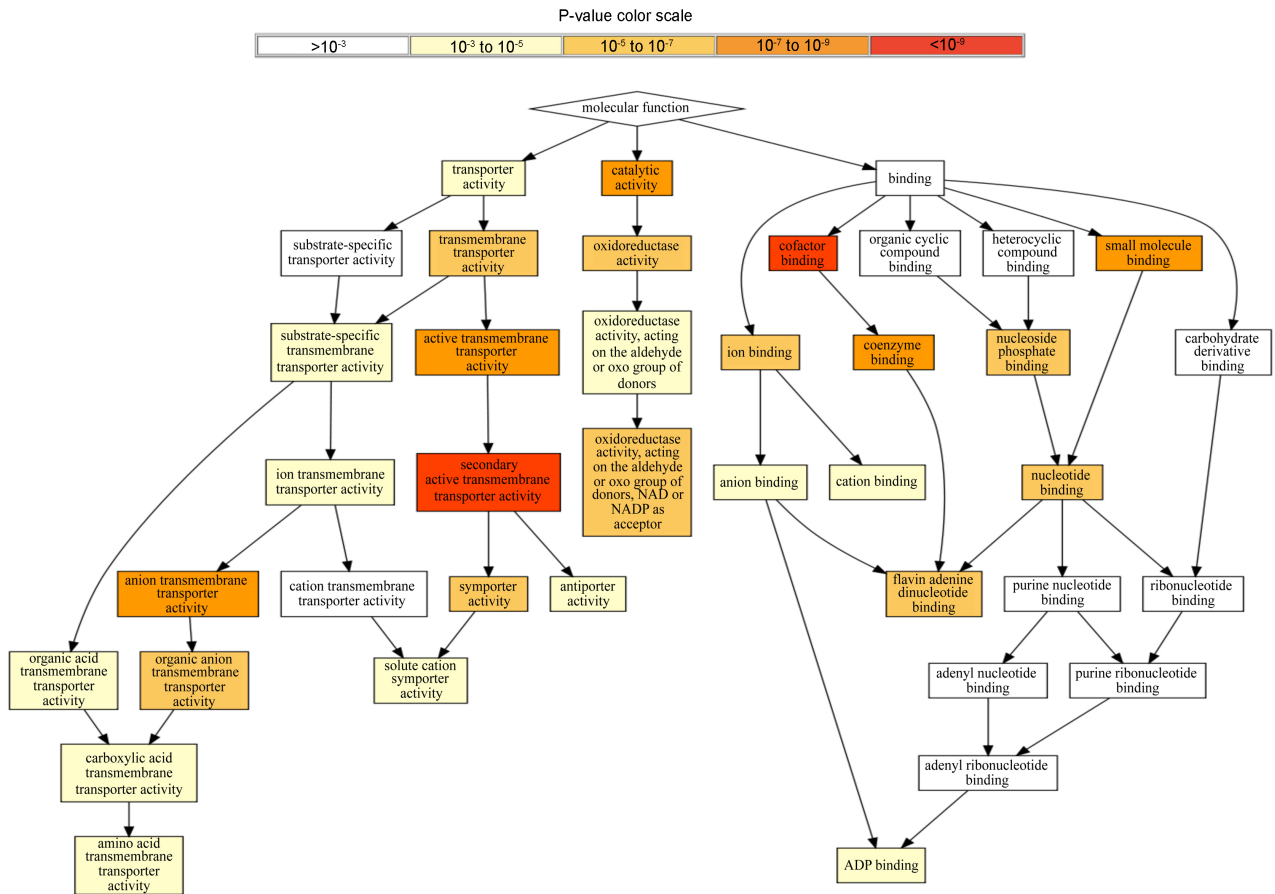


Figure 5. GO classification of enriched molecular function in renal scaffold.

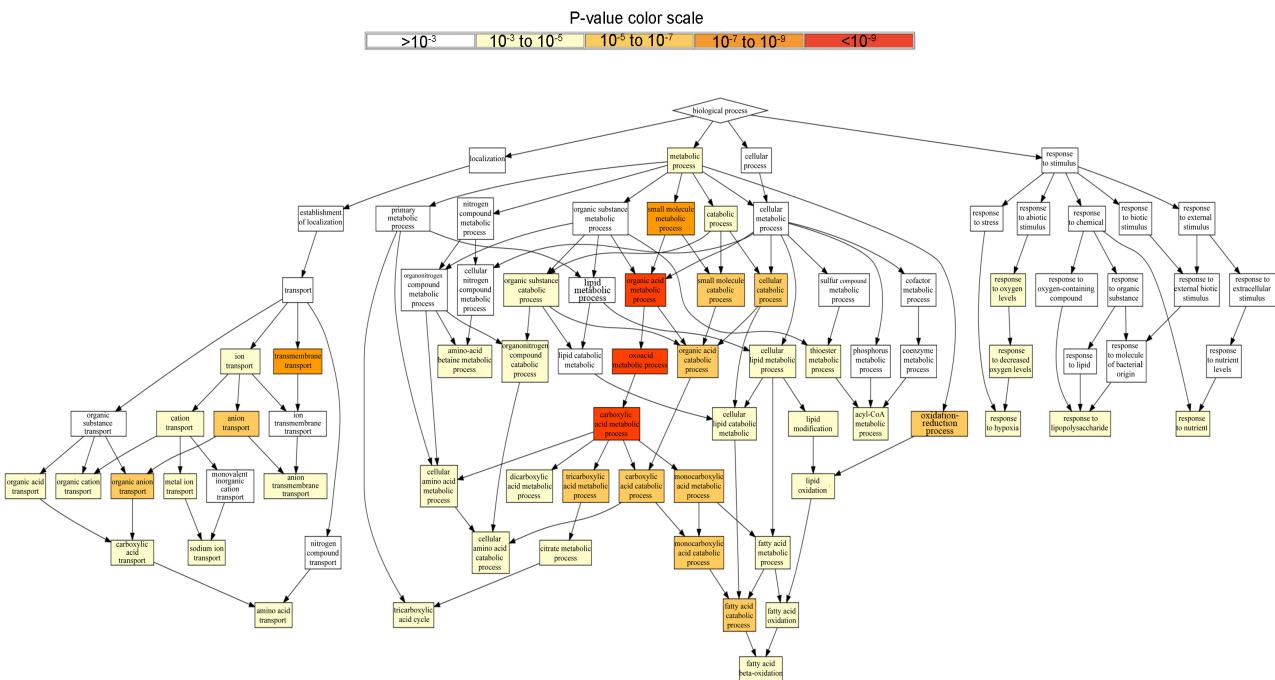


Figure 6. GO classification of enriched biological process in renal scaffold.

Table 3. GO classification of enriched molecular function.

GO term	Ontology	Description	p-Value	FDR q-value	Enrichment
GO:0048037	Molecular Function	cofactor binding	1.45E-10	2.61E-7	1.79
GO:0015291	Molecular Function	secondary active transmembrane transporter activity	5.81E-10	5.24E-7	2.43
GO:0022804	Molecular Function	active transmembrane transporter activity	4.61E-9	2.77E-6	1.99
GO:0036094	Molecular Function	small molecule binding	1.23E-8	5.55E-6	1.34
GO:0008509	Molecular Function	anion transmembrane transporter activity	4.43E-8	1.6E-5	2.26
GO:0003824	Molecular Function	catalytic activity	5.98E-8	1.79E-5	1.20
GO:0050662	Molecular Function	coenzyme binding	7.41E-8	1.91E-5	1.76
GO:0050660	Molecular Function	flavin adenine dinucleotide binding	3.07E-7	6.92E-5	2.29
GO:0008514	Molecular Function	organic anion transmembrane transporter activity	3.46E-7	6.93E-5	2.37
GO:0016491	Molecular Function	oxidoreductase activity	4.52E-7	8.15E-5	1.46
GO:1901265	Molecular Function	nucleoside phosphate binding	8.79E-7	1.44E-4	1.34
GO:0000166	Molecular Function	nucleotide binding	8.79E-7	1.32E-4	1.34
GO:0022857	Molecular Function	transmembrane transporter activity	9.03E-7	1.25E-4	1.66
GO:0016620	Molecular Function	oxidoreductase activity, acting on the aldehyde or oxo group of donors, NAD or NADP acceptor	1.31E-6	1.68E-4	2.61
GO:0043167	Molecular Function	ion binding	2.95E-6	3.54E-4	1.20
GO:0015293	Molecular Function	symporter activity	9.23E-6	1.04E-3	2.61
GO:0016903	Molecular Function	oxidoreductase activity, acting on the aldehyde or oxo group of donors	1.18E-5	1.25E-3	2.32

Continued

GO:0043531	Molecular Function	ADP binding	3.17E-5	3.17E-3	2.42
GO:0043168	Molecular Function	anion binding	3.44E-5	3.26E-3	1.25
GO:0022891	Molecular Function	substrate-specific transmembrane transporter activity	6.73E-5	6.06E-3	1.56
GO:0015075	Molecular Function	ion transmembrane transporter activity	1.16E-4	9.92E-3	1.55
GO:0005342	Molecular Function	organic acid transmembrane transporter activity	1.55E-4	1.27E-2	2.26
GO:0015171	Molecular Function	amino acid transmembrane transporter activity	4.51E-4	3.53E-2	2.61
GO:0015294	Molecular Function	solute:cation symporter activity	4.51E-4	3.38E-2	2.61
GO:0005215	Molecular Function	transporter activity	6.09E-4	4.39E-2	1.37
GO:0015297	Molecular Function	antiporter activity	8.17E-4	5.66E-2	2.21
GO:0046943	Molecular Function	carboxylic acid transmembrane transporter activity	8.17E-4	5.45E-2	2.21
GO:0043169	Molecular Function	cation binding	9.23E-4	5.94E-2	1.22

mmHg) during the entire duration of the decellularization process. This approach differs from the gravity-based perfusion system adopted by Guyette J *et al.* [11]. Moreover, we decided to use a lower concentration of SDS (0.66%), because high concentrations of SDS can lead to the destruction of the ECM [20-22]. Histological data showed that our decellularization procedure was effective in maintaining kidney microarchitecture. Furthermore, even the integrity of the basal membrane is preserved, which is a basic requirement for successful endothelialization of the vessels [23]. Recellularization process requires not only the preservation of the overall architectural integrity of the organ but the maintenance of a vascular network intact, both are indispensable for ensuring adequate oxygenation of the organ. Taking this into consideration, we demonstrated that the vascular tree was preserved after the decellularization process, which was evidenced by perfusion through renal artery of blue colored solution.

In this research, we employed a proteomics approach (by LC-MS/MS) to generate a comprehensive protein expression profile of kidney scaffold. As expected, fewer distinct proteins were detected after decellularization process. We identified 424 proteins in the kidney scaffold of which 296 proteins were conserved to both native and kidney scaffold. In the decellularized kidney scaffold, we identified a large number of both remnant cellular and ECM proteins. During creation of a decellularized scaffold, it is crucial to preserve the organ-specific ECM “zip codes” that support site appropriate cell attachment and differentiation [15, 24]. The identification of acellular matrix composition by LC-MS/MS confirms the expression of the main components of ECM including collagen type I, laminin, fibronectin, vimentin and

Table 4. GO classification of enriched biological process.

GO term	Ontology	Description	p-Value	FDR q-value	Enrichment
GO:0006082	Biological Process	organic acid metabolic process	5.18E-12	3.71E-8	1.56
GO:0043436	Biological Process	oxoacid metabolic process	1.79E-11	6.43E-8	1.55
GO:0019752	Biological Process	carboxylic acid metabolic process	6.09E-11	1.45E-7	1.54
GO:0044281	Biological Process	small molecule metabolic process	2.78E-8	4.98E-5	1.34
GO:0055085	Biological Process	transmembrane transport	8.63E-8	1.24E-4	1.67
GO:0055114	Biological Process	oxidation-reduction process	1.06E-7	1.26E-4	1.46
GO:0016054	Biological Process	organic acid catabolic process	1.34E-7	1.37E-4	1.76
GO:0046395	Biological Process	carboxylic acid catabolic process	1.34E-7	1.2E-4	1.76
GO:0006820	Biological Process	anion transport	2.4E-7	1.91E-4	1.88
GO:0072329	Biological Process	monocarboxylic acid catabolic process	5.39E-7	3.86E-4	2.04
GO:0072350	Biological Process	tricarboxylic acid metabolic process	7.28E-7	4.74E-4	2.28
GO:0032787	Biological Process	monocarboxylic acid metabolic process	1.15E-6	6.88E-4	1.57
GO:0044282	Biological Process	small molecule catabolic process	1.51E-6	8.31E-4	1.62
GO:0009062	Biological Process	fatty acid catabolic process	1.85E-6	9.47E-4	2.05
GO:0015711	Biological Process	organic anion transport	5.62E-6	2.68E-3	1.85
GO:0044248	Biological Process	cellular catabolic process	8.25E-6	3.69E-3	1.36

Continued

GO:0006635	Biological Process	fatty acid beta-oxidation	1.35E-5	5.7E-3	2.05
GO:0009056	Biological Process	catabolic process	1.72E-5	6.84E-3	1.31
GO:0006099	Biological Process	tricarboxylic acid cycle	2.13E-5	8.04E-3	2.22
GO:0006101	Biological Process	citrate metabolic process	2.13E-5	7.64E-3	2.22
GO:0034440	Biological Process	lipid oxidation	2.16E-5	7.35E-3	1.95
GO:0019395	Biological Process	fatty acid oxidation	2.16E-5	7.02E-3	1.95
GO:0006577	Biological Process	amino-acid betaine metabolic process	2.45E-5	7.61E-3	2.61
GO:0006811	Biological Process	ion transport	2.99E-5	8.92E-3	1.46
GO:0015849	Biological Process	organic acid transport	3.62E-5	1.04E-2	1.98
GO:1901565	Biological Process	organonitrogen compound catabolic process	3.86E-5	1.06E-2	1.50
GO:1901575	Biological Process	organic substance catabolic process	4.41E-5	1.17E-2	1.33
GO:0098656	Biological Process	anion transmembrane transport	4.86E-5	1.24E-2	2.19
GO:0030258	Biological Process	lipid modification	5.78E-5	1.43E-2	1.86
GO:0046942	Biological Process	carboxylic acid transport	7.41E-5	1.77E-2	1.95
GO:0044242	Biological Process	cellular lipid catabolic process	7.86E-5	1.82E-2	1.76
GO:0070482	Biological Process	response to oxygen levels	1.46E-4	3.27E-2	1.61
GO:0006865	Biological Process	amino acid transport	1.71E-4	3.71E-2	2.61
GO:0006814	Biological Process	sodium ion transport	1.92E-4	4.04E-2	2.39
GO:0030001	Biological Process	metal ion transport	2.43E-4	4.97E-2	1.76
GO:0043648	Biological Process	dicarboxylic acid metabolic process	2.61E-4	5.2E-2	1.72
GO:0036293	Biological Process	response to decreased oxygen levels	2.64E-4	5.11E-2	1.62

Continued

GO:0006631	Biological Process	fatty acid metabolic process	3.68E-4	6.93E-2	1.55
GO:0006520	Biological Process	cellular amino acid metabolic process	4.15E-4	7.63E-2	1.49
GO:0044255	Biological Process	cellular lipid metabolic process	4.23E-4	7.58E-2	1.42
GO:0001666	Biological Process	response to hypoxia	4.49E-4	7.84E-2	1.60
GO:0015695	Biological Process	organic cation transport	4.51E-4	7.69E-2	2.61
GO:0008152	Biological Process	metabolic process	4.53E-4	7.55E-2	1.10
GO:0009063	Biological Process	cellular amino acid catabolic process	4.67E-4	7.61E-2	1.69
GO:0007584	Biological Process	response to nutrient	6.79E-4	1.08E-1	1.55
GO:0032496	Biological Process	response to lipopolysaccharide	7.83E-4	1.22E-1	1.74
GO:0006637	Biological Process	acyl-CoA metabolic process	8.8E-4	1.34E-1	1.95
GO:0035383	Biological Process	thioester metabolic process	8.8E-4	1.31E-1	1.95
GO:0006812	Biological Process	cation transport	9.52E-4	1.39E-1	1.46

nidogen, among others.

Currently, the few published reports of proteome composition of decellularized biological scaffolds focus primarily on ECM proteins [15, 25-27]. In this work, along with ECM proteins, we identified numerous cellular proteins mainly related to metabolic processes, in binding and transporter activity. Interestingly, we identified proteins involved in kidney development (Slc34a1, Aqp1, Mme, Podxl, Sdc4, Nphs2, Hspa4, Cat, Hrsp12, Cyp4a8, Asl, Aldh1a1, Aldh9a1, Acat1, Ass1). Particularly, Podxl, Aqp1 and Nphs2 are involved in kidney epithelium development and glomerulus development. Specifically, Podxl play an essential role in the formation and maintenance of podocyte foot processes [28] and Podxl-deficiency prevents renal tubule formation [29].

5. CONCLUSION

Collectively, our data reveal that decellularized kidney scaffold retain characteristic cues from local microenvironment that could be the basis for specific homing and cellular differentiation in the recellularization process. Thus, we assume that the goal of decellularization is to identify the crucial proteins that must remain within the biological scaffolds in order to complete a successful recellularization process.

ACKNOWLEDGEMENTS

The authors are grateful to Dr. Ignacio Ortea from IMIBIC Proteomics Unit and M. J. Jimenez for their technical assistance.

REFERENCES

1. Schoolwerth, A.C., Engelgau, M.M., Hostetter, T.H., Rufo, K.H., Chianchiano, D., McClellan, W.M., *et al.* (2006) Chronic Kidney Disease: A Public Health Problem That Needs a Public Health Action Plan. *Preventing Chronic Disease*, **3**, A57.
2. Schieppati, A. and Remuzzi, G. (2005) Chronic Renal Diseases as a Public Health Problem: Epidemiology, Social, and Economic Implications. *Kidney International Supplements*, **98**, S7-S10. <https://doi.org/10.1111/j.1523-1755.2005.09801.x>
3. Meguid El Nahas, A. and Bello, A.K. (2005) Chronic Kidney Disease: The Global Challenge. *Lancet*, **365**, 331-340. [https://doi.org/10.1016/S0140-6736\(05\)17789-7](https://doi.org/10.1016/S0140-6736(05)17789-7)
4. Abolbashari, M., Agcaoili, S.M., Lee, M.K., Ko, I.K., Aboushwareb, T., Jackson, J.D., *et al.* (2016) Repopulation of Porcine Kidney Scaffold Using Porcine Primary Renal Cells. *Acta Biomater*, **29**, 52-61. <https://doi.org/10.1016/j.actbio.2015.11.026>
5. Ott, H.C., Matthiesen, T.S., Goh, S.K., Black, L.D., Kren, S.M., Netoff, T.I., *et al.* (2008) Perfusion-Decellularized Matrix: Using Nature's Platform to Engineer a Bioartificial Heart. *Nature Medicine*, **14**, 213-221. <https://doi.org/10.1038/nm1684>
6. Ott, H.C., Clippinger, B., Conrad, C., Schuetz, C., Pomerantseva, I., Ikonou, L., *et al.* (2010) Regeneration and Orthotopic Transplantation of a Bioartificial Lung. *Nature Medicine*, **16**, 927-933. <https://doi.org/10.1038/nm.2193>
7. Uygun, B.E., Soto-Gutierrez, A., Yagi, H., Izamis, M.L., Guzzardi, M.A., Shulman, C., *et al.* (2010) Organ Reengineering through Development of a Transplantable Recellularized Liver Graft Using Decellularized Liver Matrix. *Nature Medicine*, **16**, 814-820. <https://doi.org/10.1038/nm.2170>
8. Baptista, P.M., Siddiqui, M.M., Lozier, G., Rodriguez, S.R., Atala, A. and Soker, S. (2011) The Use of Whole Organ Decellularization for the Generation of a Vascularized Liver Organoid. *Hepatology*, **53**, 604-617. <https://doi.org/10.1002/hep.24067>
9. Orlando, G., Wood, K.J., Stratta, R.J., Yoo, J.J., Atala, A. and Soker, S. (2011) Regenerative Medicine and Organ Transplantation: Past, Present, and Future. *Transplantation*, **91**, 1310-1317. <https://doi.org/10.1097/TP.0b013e318219ebb5>
10. Chani, B., Puri, V., Sobti, R.C., Jha, V. and Puri, S. (2017) Decellularized Scaffold of Cryopreserved Rat Kidney Retains Its Recellularization Potential. *PLoS One*, **12**, e0173040. <https://doi.org/10.1371/journal.pone.0173040>
11. Guyette, J.P., Gilpin, S.E., Charest, J.M., Tapias, L.F., Ren, X. and Ott, H.C. (2014) Perfusion Decellularization of Whole Organs. *Nature Protocols*, **9**, 1451-1468. <https://doi.org/10.1038/nprot.2014.097>
12. Peloso, A., Ferrario, J., Maiga, B., Benzoni, I., Bianco, C., Citro, A., *et al.* (2015) Creation and Implantation of Acellular Rat Renal ECM-Based Scaffolds. *Organogenesis*, **11**, 58-74. <https://doi.org/10.1080/15476278.2015.1072661>
13. Song, J.J., Guyette, J.P., Gilpin, S.E., Gonzalez, G., Vacanti, J.P. and Ott, H.C. (2013) Regeneration and Experimental Orthotopic Transplantation of a Bioengineered Kidney. *Nature Medicine*, **19**, 646-651. <https://doi.org/10.1038/nm.3154>
14. Caralt, M., Uzarski, J.S., Jacob, S., Oberfell, K.P., Berg, N., Bijonowski, B.M., *et al.* (2015) Optimization and Critical Evaluation of Decellularization Strategies to Develop Renal Extracellular Matrix Scaffolds as Biological Templates for Organ Engineering and Transplantation. *American Journal of Transplantation*, **15**, 64-75.

<https://doi.org/10.1111/ajt.12999>

15. Li, Q., Uygun, B.E., Geerts, S., Oze, S., Scalf, M., Gilpin, S.E., *et al.* (2016) Proteomic Analysis of Naturally-Sourced Biological Scaffolds. *Biomaterials*, **75**, 37-46. <https://doi.org/10.1016/j.biomaterials.2015.10.011>
16. Rusconi, F., Valton, E., Nguyen, R. and Dufourc, E. (2001) Quantification of Sodium Dodecyl Sulfate in Micro-liter-Volume Biochemical Samples by Visible Light Spectroscopy. *Analytical Biochemistry*, **295**, 31-37. <https://doi.org/10.1006/abio.2001.5164>
17. Vowinckel, J., Capuano, F., Campbell, K., Deery, M.J., Lilley, K.S. and Ralser, M. (2013) The Beauty of Being (label)-Free: Sample Preparation Methods for SWATH-MS and Next-Generation Targeted Proteomics. *F1000Research*, **2**, 272. <https://doi.org/10.12688/f1000research.2-272.v2>
18. Wang, Y., Bao, J., Wu, Q., Zhou, Y., Li, Y., Wu, X., *et al.* (2015) Method for Perfusion Decellularization of Porcine Whole Liver and Kidney for Use as a Scaffold for Clinical-Scale Bioengineering Engrafts. *Xenotransplantation*, **22**, 48-61. <https://doi.org/10.1111/xen.12141>
19. Destefani, A.C., Sirtoli, G.M. and Nogueira, B.V. (2017) Advances in the Knowledge about Kidney Decellularization and Repopulation. *Frontiers in Bioengineering and Biotechnology*, **5**, 34. <https://doi.org/10.3389/fbioe.2017.00034>
20. Samouillan, V., Dandurand-Lods, J., Lamure, A., Maurel, E., Lacabanne, C., Gerosa, G., *et al.* (1999) Thermal Analysis Characterization of Aortic Tissues for Cardiac Valve Bioprostheses. *Journal of Biomedical Materials Research*, **46**, 531-538. [https://doi.org/10.1002/\(SICI\)1097-4636\(19990915\)46:4<531::AID-JBM11>3.0.CO;2-2](https://doi.org/10.1002/(SICI)1097-4636(19990915)46:4<531::AID-JBM11>3.0.CO;2-2)
21. Woods, T. and Gratzner, P.F. (2005) Effectiveness of Three Extraction Techniques in the Development of a Decellularized Bone-Anterior Cruciate Ligament-Bone Graft. *Biomaterials*, **26**, 7339-7349. <https://doi.org/10.1016/j.biomaterials.2005.05.066>
22. Ren, H., Shi, X., Tao, L., Xiao, J., Han, B., Zhang, Y., *et al.* (2013) Evaluation of Two Decellularization Methods in the Development of a Whole-Organ Decellularized Rat Liver Scaffold. *Liver International*, **33**, 448-458. <https://doi.org/10.1111/liv.12088>
23. Ross, E.A., Williams, M.J., Hamazaki, T., Terada, N., Clapp, W.L., Adin, C., *et al.* (2009) Embryonic Stem Cells Proliferate and Differentiate When Seeded into Kidney Scaffolds. *Journal of the American Society of Nephrology*, **20**, 2338-2347. <https://doi.org/10.1681/ASN.2008111196>
24. Crapo, P.M., Gilbert, T.W. and Badylak, S.F. (2011) An Overview of Tissue and Whole Organ Decellularization Processes. *Biomaterials*, **32**, 3233-3243. <https://doi.org/10.1016/j.biomaterials.2011.01.057>
25. Gilpin, S.E., Guyette, J.P., Gonzalez, G., Ren, X., Asara, J.M., Mathisen, D.J., *et al.* (2014) Perfusion Decellularization of Human and Porcine Lungs: Bringing the Matrix to Clinical Scale. *The Journal of Heart and Lung Transplantation*, **33**, 298-308. <https://doi.org/10.1016/j.healun.2013.10.030>
26. Marçal, H., Ahmed, T., Badylak, S.F., Tottey, S. and Foster, L.J. (2012) A Comprehensive Protein Expression Profile of Extracellular Matrix Biomaterial Derived from Porcine Urinary Bladder. *Regenerative Medicine*, **7**, 159-166. <https://doi.org/10.2217/rme.12.6>
27. Hill, R.C., Calle, E.A., Dzieciatkowska, M., Niklason, L.E. and Hansen, K.C. (2015) Quantification of Extracellular Matrix Proteins from a Rat Lung Scaffold to Provide a Molecular Readout for Tissue Engineering. *Molecular & Cellular Proteomics*, **14**, 961-973. <https://doi.org/10.1074/mcp.M114.045260>
28. Doyonnas, R., Kershaw, D.B., Duhme, C., Merckens, H., Chelliah, S., Graf, T., *et al.* (2001) Anuria, Omphalocele, and Perinatal Lethality in Mice Lacking the CD34-Related Protein Podocalyxin. *The Journal of Experimental Medicine*, **194**, 13-27. <https://doi.org/10.1084/jem.194.1.13>
29. Cheng, H.Y., Lin, Y.Y., Yu, C.Y., Chen, J.Y., Shen, K.F., Lin, W.L., *et al.* (2005) Molecular Identification of Ca-

nine Podocalyxin-Like Protein 1 as a Renal Tubulogenic Regulator. *Journal of the American Society of Nephrology*, **16**, 1612-1622. <https://doi.org/10.1681/ASN.2004121145>

SUPPLEMENTARY INFORMATION IS AVAILABLE AT:

<https://1drv.ms/x/s!AGhdhjFEC73rg1Y>